JANUSZ CEBULSKI
ORCID: 0000-0002-3813-8705

Silesian University of Technology, Faculty of Materials Engineering, Katowice, Poland

DOI: 10.15199/40.2023.5.2

High-temperature oxidation of $Fe_{40}Al_5Cr_{0.2}TiB$ intermetallic phase-based alloy depending on its surface condition

Wysokotemperaturowe utlenianie stopu na osnowie fazy międzymetalicznej $Fe_{40}Al_5Cr_{0,2}TiB$ w zależności od stanu powierzchni

The influence of an FeAl intermetallic phase-based alloy's surface condition on the high-temperature corrosion process during annealing in air at 1000°C for 500 h was investigated. The structure of the oxide scale was determined and related to the initial surface condition before the oxidation process. Oxidation was observed using a Hitachi S-4200 scanning electron microscope. X-ray microanalysis of the chemical composition (EDS) was also carried out for all the tested samples after oxidation. The relationship between the structure of the oxide scale layer and the type of surface before oxidation was demonstrated.

Keywords: FeAl alloys, high-temperature corrosion, scale, Al_2O_3 oxide

W pracy dokonano analizy wpływu stanu powierzchni na przebieg procesu korozji wysokotemperaturowej stopu na osnowie fazy międzymetalicznej FeAl podczas wyżarzania w powietrzu w temperaturze 1000°C przez 500 h. Określono budowę zgorzeliny tlenkowej i odniesiono te dane do stanu powierzchni przed procesem utleniania. Próbki po procesie utleniania obserwowano przy użyciu elektronowego mikroskopu skaningowego Hitachi S-4200. Przeprowadzono również mikroanalizę rentgenowską składu chemicznego (EDS) wszystkich badanych próbek po utlenianiu. Wykazano zależność pomiędzy budową warstwy zgorzeliny tlenkowej a rodzajem powierzchni przed utlenianiem.

Słowa kluczowe: stopy FeAl, korozja wysokotemperaturowa, zgorzelina, tlenek Al_2O_3

1. Introduction

The continuous development of the world economy in terms of new technologies, the production of elements with increasingly better properties, and decreasing production costs all pose a significant challenge in the development of materials with the best set of features. The development of materials engineering in the scope of testing alloys based on intermetallic phases has contributed to an increase in the range of their practical applications in various industries [1, 2].

Intermetallic phase matrix alloys have proven to be a good substitute, which in the future may replace some of the currently used materials intended for operation in high-temperature corrosion environments. This applies, among others, to steels, especially high-alloy or nickel-based alloys. For this reason in particular, intermetallic alloys have found application in a wide range of industrial, chemical, petrochemical, aviation and automotive industries. A positive aspect that significantly influenced the use of these alloys on such a wide scale is the relatively low cost of input materials used for the production of alloys based on the FeAl intermetallic phase [1–3].

These alloys show good corrosion resistance at elevated temperatures in air, but also in water vapor [3–7]. This resistance is related to the formation of a passive protective layer of Al_2O_3 oxide on the surface of the alloy. The compact structure forms a barrier against oxygen diffusion inside the core, which ensures protection against high-temperature corrosion [5].

Research on the properties of alloys based on the FeAl phase, improvement of their production methods, assessment of the strength of these alloys under the action of various factors are in a continuous phase of development. Numerous studies and the resulting modifications of alloys result in an improvement in the properties of intermetallics [6–10].

2. Research methodology

The test material consisted of samples 22 mm × 10 mm in size made of $Fe_{40}Al_5Cr_{0.2}TiB$ alloy (Table 1). Melting of the material was carried out in an induction vacuum furnace VSG (Balzers). The following pure ingredients were used for the smelting process: technically pure armco iron and aro aluminum with a purity of 99.99% by weight. Before the oxidation process, the surface process was prepared in three variants: after electro-spark cutting, polishing with 1 μm paste and grinding with 500 grit paper. The tests included an analysis of scale morphology and the surface condition of $Fe_{40}Al_5Cr_{0.2}TiB$ alloy samples. The material after polishing was used as a reference as it exhibited the most homogeneous layer of the scale.

Janusz Cebulski, BEng, PhD, is a graduate of the Faculty of Materials Engineering, Metallurgy, Transport and Management of the Silesian University of Technology. He works as an assistant professor at the Faculty of Materials Science and Metallurgy at the Silesian University of Technology. His areas of research interest include alloys based on intermetallic compounds, in particular from the Fe–Al system, material structure studies, scanning electron microscopy, and cracking of materials.

E-mail: janusz.cebulski@polsl.pl

Otrzymano / Received: 13.03.2023. Przyjęto / Accepted: 30.03.2023

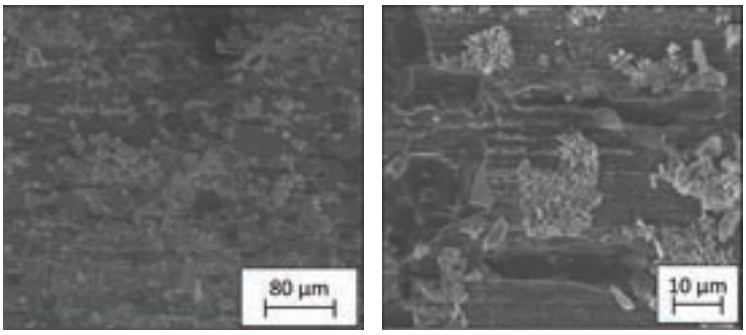

Fig. 1. Surface of $Fe_{40}Al_5Cr_{0.2}TiB$ alloy after electro-spark cutting and high-temperature corrosion for 500 h at 1000°C

Rys. 1. Powierzchnia stopu $Fe_{40}Al_5Cr_{0,2}TiB$ po cięciu elektroiskrowym i korozji wysokotemperaturowej w czasie 500 h w temperaturze 1000°C

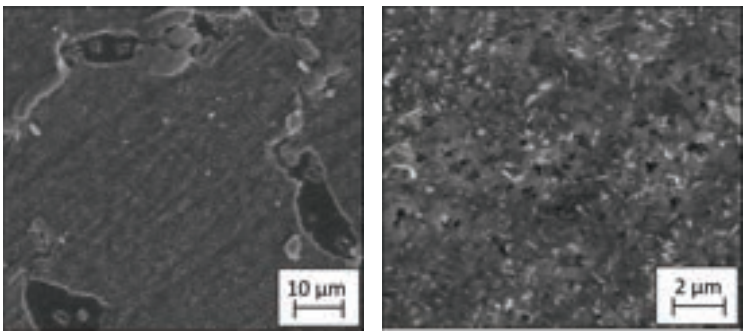

Fig. 2. Surface of $Fe_{40}Al_5Cr_{0.2}TiB$ alloy after polishing and high-temperature corrosion for 500 h at 1000°C

Rys. 2. Powierzchnia stopu $Fe_{40}Al_5Cr_{0,2}TiB$ po procesie polerowania i korozji wysokotemperaturowej w czasie 500 h w temperaturze 1000°C

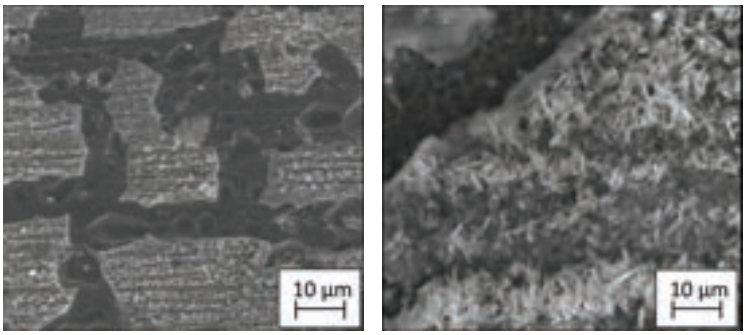

Fig. 3. Surface of $Fe_{40}Al_5Cr_{0.2}TiB$ alloy after grinding with 500 grit paper and high-temperature corrosion for 500 h at 1000°C

Rys. 3. Powierzchnia stopu $Fe_{40}Al_5Cr_{0,2}TiB$ po procesie szlifowania papierem o gradacji 500 i korozji wysokotemperaturowej w czasie 500 h w temperaturze 1000°C

Research methodology:

- Oxidation in a Carbolite oven at 1000°C for 500 h.
- Observation with a Hitachi S-4200 field emission scanning electron microscope. The observation was carried out at an accelerating voltage of 20 kV, while the tests were carried out on samples after the oxidation process.
- The study of the chemical composition was carried out using a Thermo Noran energy dispersive X-ray spectrometer (EDS) at 15 keV primary beam energy. This spectrometer was coupled with a Hitachi S-4200 scanning electron microscope.

Table 1. Chemical composition of $Fe_{40}Al_5Cr_{0.2}TiB$ alloy
Tabela 1. Skład chemiczny stopu $Fe_{40}Al_5Cr_{0,2}TiB$

Alloy/Stop	Chemical composition, mass %/Skład chemiczny, % mas.				
	Fe	Al	Cr	Ti	B
$Fe_{40}Al_5Cr_{0.2}TiB$	68.22	23.69	5.69	0.19	0.015

3. Results of experimental research

3.1. Morphology of the alloy surface after oxidation

Observations carried out using a scanning electron microscope made it possible to determine the morphology of oxidation products formed on the surface of the tested alloy [11]. The sample subjected to electro-spark cutting after the oxidation process (Fig. 1) was characterized by a scale with a heterogeneous surface. On the surface of the alloy, places of scale layer chipping are visible. The oxide on the surface of the FeAl alloy is grouped in the form of needles (Fig. 1b).

The sample subjected to polishing after oxidation (Fig. 2) is characterized by a uniform layer of scale. There are visible places where chipping of the oxide layer took place, however, relatively few of them can be found. The morphology of the formed oxides, visible in Fig. 2b, illustrates the presence of a few oxide needles, predominantly in the form of lumps and lamellar grains.

The surface of the sample ground with 500 grit paper, after oxidation (Fig. 3), is characterized by the presence of numerous locations where the scale has crumbled. The morphology of the formed oxide (Fig. 3b) shows a mainly acicular structure with a few plates.

3.2. Chemical composition of corrosion products

After oxidation at 1000°C/500 h, the surface of the oxidized layer (Fig. 4) differed in terms of its chemical composition. The presence of areas covered with a tarnished layer of aluminum oxide and areas with oxides in the form of needles or lumps was found. EDS tests confirmed the presence of iron, aluminum and chromium in the material in which the oxide layer detached. Only aluminum and oxygen were found among the oxidation products

a)

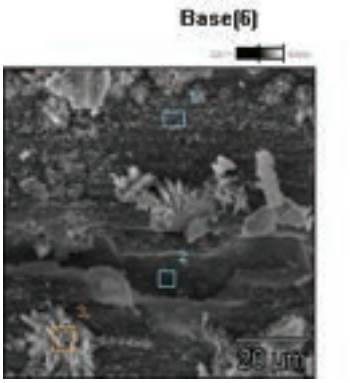

b)

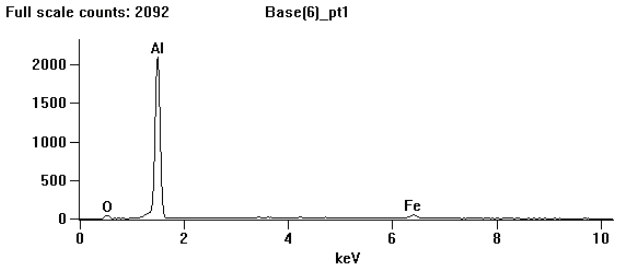

c)

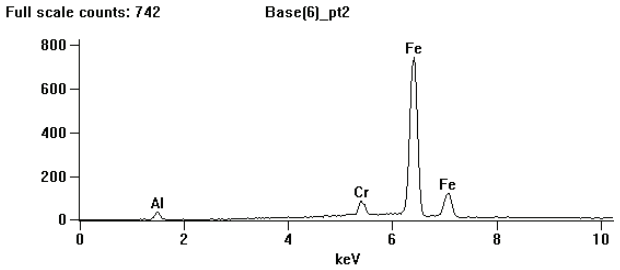

d)

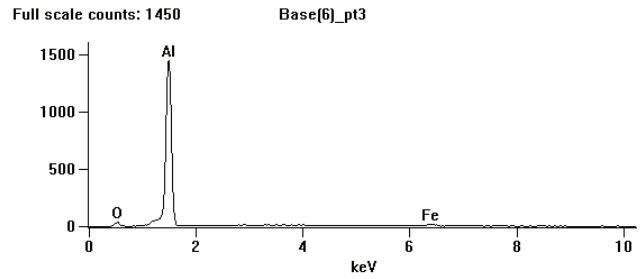

e)

Atom. %	O	Al	Cr	Fe
pt1	19.5	76.7	–	3.8
pt2	–	5.8	3.9	90.2
pt3	21.9	75.6	–	2.5

Fig. 4. Surface morphology of $Fe_{40}Al_5Cr_{0.2}TiB$ alloy for a sample after electro-spark cutting and high-temperature corrosion at 1000°C/500 h with marked areas for X-ray microanalysis (a); X-ray spectra with energy dispersion (EDS) from the places marked in Fig. 4a (b–d); chemical composition of marked areas (e)

Rys. 4. Morfologia powierzchni stopu $Fe_{40}Al_5Cr_{0.2}TiB$ w próbce po cięciu elektroiskrowym i korozji wysokotemperaturowej 1000°C/500 h z zaznaczonymi obszarami do mikroanalizy rentgenowskiej (a); widma promieniowania rentgenowskiego z dyspersją energii (EDS) z miejsc zaznaczonych na rys. 4a (b–d); skład chemiczny zaznaczonych obszarów (e)

for all surface conditions, which proves the selective oxidation of the alloy with the corrosion product being aluminum oxide.

4. Summary

Analysis of the obtained test results allows us to conclude that the surface, after polishing, is characterized by the most homogeneous scale structure. Compared to other variants of the samples, the polished surface featured few locations of scale detachment. The reason for the detachment of the oxide layer from the surface of the tested material may be the stress caused by the cooling process of the tested samples, which then leads to the crushing of the scale layer [5, 12]. Crushing of the scale from the surface of the tested samples is also related to its adhesion to the substrate, a fact also confirmed in study [13]. Assessment of the morphology of the oxides formed indicates that the least homogeneous scale surface is characteristic of the sample subjected to electro-spark cutting. For all variants of the samples, the presence of chipped scale fragments was observed on the surface. The sample ground with 500 grit paper is characterized by the highest number of scale-free locations. Compressive stresses arising in the oxide are responsible for the formation of needles referred to as "whiskers" [14]. The surface subjected to electro-spark cutting is characterized by the presence of the greatest number of needles compared to the rest of the tested samples. Differences in the size of the needles

a)

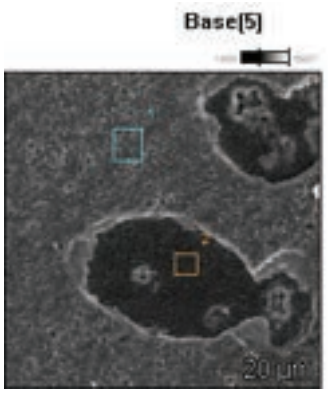

b)

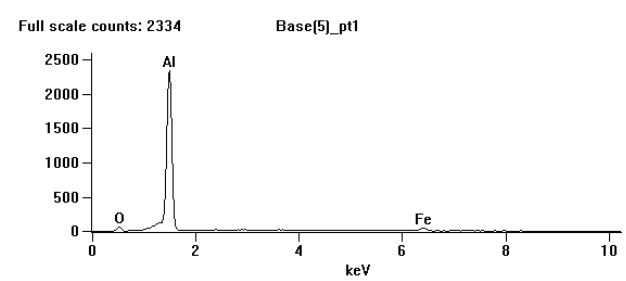

c)

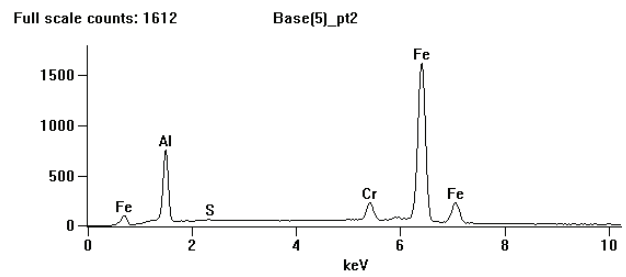

d)

Atom. %	O	Al	Ti	Cr	Fe
pt1	–	33.4	–	2.9	63.8
pt2	25.2	71.7	0.1	–	3.0

Fig. 5. Surface morphology of $Fe_{40}Al_5Cr_{0.2}TiB$ alloy for a sample after polishing and high-temperature corrosion at 1000°C/500 h with marked areas for X-ray microanalysis (a); X-ray spectra with energy dispersion (EDS) from places marked in Fig. 5a (b, c); chemical composition of marked areas (d)

Rys. 5. Morfologia powierzchni stopu $Fe_{40}Al_5Cr_{0.2}TiB$ w próbce po polerowaniu i korozji wysokotemperaturowej 1000°C/500 h z zaznaczonymi obszarami do mikroanalizy rentgenowskiej (a); widma promieniowania rentgenowskiego z dyspersją energii (EDS) z miejsc zaznaczonych na rys. 5a (b, c); skład chemiczny zaznaczonych obszarów (d)

a)

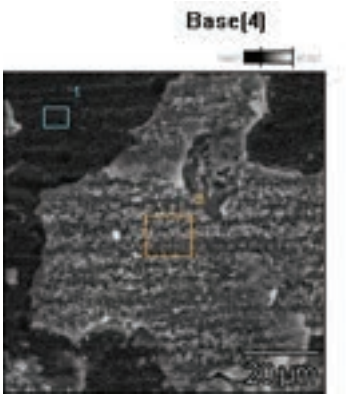

b)

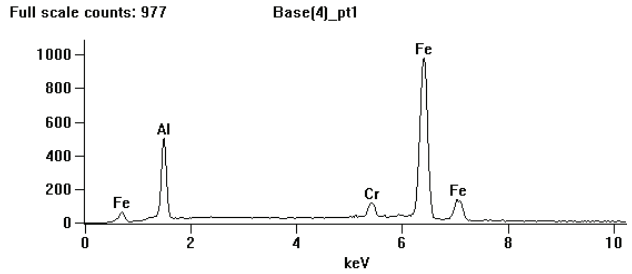

c)

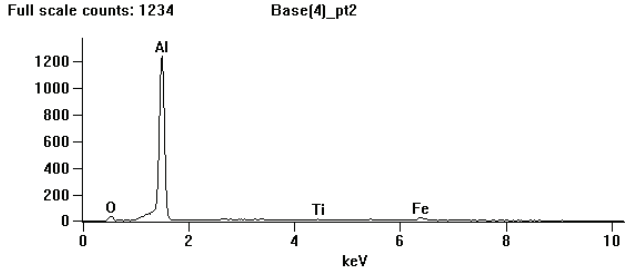

d)

Atom. %	O	Al	Ti	Cr	Fe
pt1	–	33.4	–	2.9	63.8
pt2	25.2	71.7	0.1	–	3.0

Fig. 6. Surface morphology of $Fe_{40}Al_5Cr_{0.2}TiB$ alloy for a sample ground with 500 grit sandpaper and subjected to 1000°C/500 h high-temperature corrosion with marked areas for X-ray microanalysis (a); X-ray spectra with energy dispersion (EDS) from places marked in Fig. 6a (b, c); chemical composition of marked areas (d)

Rys. 6. Morfologia powierzchni stopu $Fe_{40}Al_5Cr_{0,2}TiB$ w próbce poddanej szlifowaniu papierem ściernym o gradacji 500 i korozji wysokotemperaturowej 1000°C/500 h z zaznaczonymi obszarami do mikroanalizy rentgenowskiej (a); widma promieniowania rentgenowskiego z dyspersją energii (EDS) z miejsc zaznaczonych na rys. 6a (b, c); skład chemiczny zaznaczonych obszarów (d)

formed on the electro-spark cut surface and on other variants is the result of the oxidation reaction intensity [13, 15]. Analysis of the EDS chemical composition of the tested samples, carried out on the $Fe_{40}Al_5Cr_{0.2}TiB$ alloy, showed surface differentiation resulting from the local detachment of the oxide layer.

5. Conclusions

Based on the conducted research and results analysis, the following conclusions have been formulated:

1. Oxidation was most intensive for the sample with a surface obtained by electro-spark cutting, while high-temperature corrosion was the slowest for the sample with the polished surface.
2. The sample subjected to grinding with 500 grit paper is characterized by a relatively homogeneous structure of scale with a few detachment points that occurred as a result of thermal stresses formed during the temperature change in the cooling process.
3. The original state of the tested samples' surfaces affected the morphology of the formed Al_2O_3, and therefore the corrosion process as well as the passivation of the surface; the more homogeneous the surface, as in the case of polishing, the better the corrosion protection with a compact Al_2O_3 layer.
4. Generally, it was shown that selective oxidation of aluminum takes place on multi-component $Fe_{40}Al_5Cr_{0.2}TiB$ alloy with an FeAl intermetallic phase.

The article presents the results of research obtained in the master's thesis written by Natalia Piwowar entitled *Influence of surface condition on the course of high-temperature corrosion of alloy on FeAl intermetallic phase matrix* prepared under the supervision of the author of the publication and defended in November 2022.

BIBLIOGRAPHY

[1] Chi-Feng Lin, Toa-Hsing Chen, Yan-Wein Yang. 2020. "Effects of Niobium Addition on Dynamic Mechanical Behavior and Fracture Properties of Iron--Aluminide-Based Alloys". *Journal of Materials Research and Technology* 20: 4137–4147. DOI 10.1016/j.jmrt.2022.08.145.

[2] S. Dymek. 1998. „Charakterystyka wysokotemperaturowych związków międzymetalicznych". *Hutnik – Wiadomości Hutnicze* 6: 208–223.

[3] J. Cebulski, D. Pasek, M. Bik, K. Świerczek, P. Jeleń, K. Mroczka, J. Dąbrowa, M. Zajusz, J. Wyrwa, M. Sitarz. 2020. "*In-Situ* XRD Investigations of FeAl Intermetallic Phase-Based Alloy Oxidation". *Corrosion Science* 164: 108344. DOI: 10.1016/j.corsci.2019.108344.

[4] E.P. George, M.J. Mills, M. Yamaguchi (eds.). 1999. *High-Temperature Ordered Intermetallic Alloys VIII*: vol. 552. Cambridge University Press.

[5] D. Pasek. 2021. *Utlenianie stopu na osnowie fazy międzymetalicznej FeAl w powietrzu i parze wodnej*. Rozprawa doktorska. Katowice: Politechnika Śląska.

[6] Kang Yuan, R. Eriksson, Ru Lin Peng, Xin-Hai Li, S. Johansson, Yan-Dong Wang. 2014. "MCrAlY Coating Design Based on Oxidation-Diffusion Modelling. Part I: Microstructural Evolution". *Surface and Coatings Technology* 254: 79–96. DOI: 10.1016/j.surfcoat.2014.05.067.

[7] E. Godlewska, R. Mania, S. Szczepanik. 1999. "Selected Properties of Fe-Al Intermetallics Prepared by Various Processing Routes". *Proceedings of International Conference on Environmental Degradation of Engineering Materials*. Gdańsk–Jurata.

[8] Z. Bojar, W. Przetakiewicz (red.). 2006. *Materiały metalowe z udziałem faz międzymetalicznych*. Warszawa: Bel Studio.

[9] O. Kubaschewski. 1982. *IRON – Binary Phase Diagrams*. Berlin–Heidelberg: Springer-Verlag.

[10] S. Jóźwiak. 2014. *Aluminki żelaza. Sekwencja przemian fazowych w procesie nieizotermicznego spiekania proszków żelaza i aluminium*. Warszawa: Bel Studio.

[11] N. Piwowar. 2022. *Influence of Surface Condition on the Course of High-Temperature Corrosion of Alloy on FeAl Intermetallic Phase Matrix*. Master's thesis. Katowice: Silesian University of Technology, Faculty of Materials Engineering.

[12] H.M. Hindam, W.W. Smeltzer. 1980. "Growth and Microstructure of α-Al_2O_3 on Ni-Al alloys: Internal 27 Precipitation and Transition to External Scale". *Journal of the Electrochemical Society* 127(7): 1630–1635.

[13] D. Serafin. 2021. *Wpływ mechanicznego przygotowania powierzchni na kinetykę utleniania wysokotemperaturowego układów jedno- i dwuskładnikowych*. Rozprawa doktorska. Rzeszów: Politechnika Rzeszowska.

[14] E. Pocheć, S. Jóźwiak, K. Karczewski, Z. Bojar Z. 2011. "Fe-Al Phase Formation around SHS Reactions under Isothermal Conditions". *Journal of Alloys and Compounds* 509: 1124–1128. DOI: 10.1016/j.jallcom.2010.08.074.

[15] M. Homa. 2008. „Żaroodporność i żarowytrzymałość stali typu Fe-Cr-Al w warunkach utleniających; aktualny stan i perspektywy badań". *Prace Instytutu Odlewnictwa* 48(3): 57–85.